**Atmospheric
Chemistry
and Physics**

On the interpretation of an unusual in-situ measured ice crystal scattering phase function

A. J. Baran[1], J.-F. Gayet[2], and V. Shcherbakov[2,3]

[1]Met Office, FitzRoy Road, Exeter, EX1 3PB, UK
[2]Laboratoire de Météorologie Physique, UMR6016 CNRS/Université Blaise Pascal, Clermont-Ferrand, France
[3]Laboratoire de Météorologie Physique, Institut Universitaire de Technologie d'Allier, Montluçon, France

Correspondence to: A. J. Baran (anthony.baran@metoffice.gov.uk)

Abstract. In-situ Polar Nephelometer (PN) measurements of unusual ice crystal scattering phase functions, obtained near the cloud-top of a mid-latitude anvil cloud, at a temperature of about −58 °C, were recently reported by Gayet et al. (2012). The ice crystal habits that produced the phase functions consisted of aggregates of ice crystals and aggregates of quasi-spherical ice particles. The diameters of the individual quasi-spherical ice particles were estimated to be between about 15 µm and 20 µm. The measured-averaged scattering phase functions were featureless, at scattering angles less than about 100°, but an ice bow-like feature was noted between the scattering angles of about 120° to 160°. The estimated asymmetry parameter was 0.78 ± 0.04.

In this paper, the averaged scattering phase function is interpreted in terms of a weighted habit mixture model. The model that provides the best overall fit to the measured scattering phase function comprises of highly distorted ten-element hexagonal ice aggregates and quasi-spherical ice particles. The smaller quasi-spherical ice crystals are represented by Chebyshev ice particles of order 3, and were assumed to have equivalent spherical diameters of 24 µm. The asymmetry parameter of the best overall model was found to be 0.79. It is argued that the Chebyshev-like ice particles are responsible for the ice bow-like feature and mostly dominate the scattered intensity measured by the PN. The results from this paper have important implications for climate modelling (energy balance of anvils), cloud physics and the remote sensing of cirrus properties.

1 Introduction

The most-recent report of the Intergovernmental Panel on Climate Change (IPCC, 2007) concluded that radiative coupling, between clouds of all types, and the Earth's atmosphere is still one of the greatest uncertainties in predicting climate change. One such cloud-type that exacerbates this uncertainty is cirrus. This is because cirrus is composed of highly irregular ice crystals, which generally exist as various habit mixtures, and their sizes can vary between less than 10 µm toward the cloud-top, to several centimetres toward the cloud-bottom (Korolev et al., 2006; Baran, 2009).

Due to this variability in ice crystal size and shape, using climate models to predict the radiative effect of cirrus has proven to be problematic (Zhang et al., 1999; Kristjánsson et al., 2000; Edwards et al., 2007; Gu et al., 2011, Baran 2012). These modelling studies have shown that the net radiative effect of cirrus can be neutral, negative (i.e., cools the Earth's surface) or positive (i.e., warms the Earth's surface). The short-wave radiative effect can vary from about −30 W m^{-2} to about −70 W m^{-2} depending on model assumptions (Baran, 2009). This large range in the short-wave radiative effect is due to the uncertainty in the scattering properties of ice crystals (Baran, 2004, 2009; Ulanowski et al., 2006; Fu, 2007; Yang et al., 2008; Gayet et al., 2011, 2012). However, in recent years there has been a large amount of research that has focused on habit mixture models of cirrus and their bulk-scattering properties (Macke et al., 1996a; Mishchenko et al., 2002; McFarquhar et al., 2002; Baum et al., 2005, 2011; Baran and Labonnote, 2007; Baran 2012, and references therein).

Clearly, to improve cirrus parameterization in climate models, understanding the scattering properties of highly irregular ice crystals is of paramount importance, if the uncertainty about the net radiative effect of cirrus is to be reduced. However, such understanding is not only important for climate models but also for the space-based remote sensing of cirrus properties (Mishchenko et al., 1996; Baran et al., 1999; Yang et al., 2008; McFarlane et al., 2005; Ulanowski et al., 2011).

One scattering property that is of fundamental importance in the remote sensing of cirrus microphysical and macrophysical properties is the scattering phase function (i.e., the angle-dependent scattered intensity about the ice crystal) (van de Hulst, 1957). Application of an inappropriate phase function can lead to significant errors in the retrieval of optical thickness and/or ice crystal size (Mishchenko et al., 1996; Baran et al., 1999; Yang et al., 2008). Therefore, there is a need to constrain the scattering phase function of cirrus.

Of importance to climate models is the asymmetry parameter, which is a parameterization of the scattering phase function. The asymmetry parameter, g, is formally defined as the average cosine of the polar (scattering) angle, and is therefore, a measure of the degree of asymmetry in the forward scattering part of the phase function. The asymmetry parameter can take on, at least mathematically, values between ± 1.0. The reason why the asymmetry parameter is important for a climate model is because it is one of the scattering parameters that controls how much incident solar radiation is reflected back to space (Stephens and Webster, 1981; Liou and Takano, 1994; Baran, 2004; Ulanowski et al., 2006). Clearly, for the case of conservative scattering, high and low values of the asymmetry parameter will, respectively, reflect less and more incident solar radiation back to space. Therefore, constraining the asymmetry parameter is also just as important as constraining the scattering phase function.

Currently, passive radiometric observational evidence suggests that the best scattering phase functions to represent the radiative properties of cirrus, at solar wavelengths, are those which are featureless and relatively flat at backscattering angles (Foot, 1988; Francis et al., 1999; Baran et al., 1999, 2001; Labonnote et al., 2001; Jourdan et al., 2003; Baran and Labonnote, 2006, 2007; Baum et al., 2011). However, Gayet et al. (2012) reported the in-situ measurement of unusual ice crystal scattering phase functions, in a mid-latitude anvil cloud, towards the cloud-top, at temperatures of about $-58\,°$C. The habits responsible for the measured phase function consisted of chain-like aggregates, which consisted of non-spherical ice crystals and quasi-spherical ice particles. The chains of quasi-spherical ice particles were reported to be up to several hundred microns in length, and individual quasi-spherical particles that made up the chain were estimated to have diameters between about $15\,\mu$m and $20\,\mu$m.

The phase functions reported by Gayet et al. (2012) are unusual in that they lack any features at scattering angles less than about $100°$, but had an ice bow-like feature between the scattering angles of about $120°$ to $160°$. Therefore, this measured in-situ phase function was not relatively flat at backscattering angles. Although, this one case cannot be generalized, it does, however, demonstrate that naturally-occurring phase functions may not always be relatively flat at backscattering angles, even if halos are absent. Clearly, further measurements of naturally-occurring ice crystal scattering phase functions are needed, in different types of cirrus, in order to establish whether the occurrence of structure in the back scattering direction is common or not.

In this paper, the phase function reported by Gayet et al. (2012) is theoretically interpreted in terms of a best-fit habit mixture model of ice crystals. The paper is split into the following sections. Section 2 gives a brief discussion of the original measurements. Section 3 describes the theoretical methodology used to interpret the PN measurements, and Sect. 4 discusses the results. Section 5 presents the conclusions.

2 The measurements

In this paper, the ice crystal scattering phase function measurements reported by Gayet et al. (2012) are used, and in that paper they are comprehensibly described. However, a very brief description of the most pertinent measurements to this paper is given. The measurements were obtained during the CIRCLE-2 experiment, which was carried out over Western Europe during May 2007. During this experiment, combinations of in-situ microphysical and remote-sensing measurements were obtained in, and above, an overshooting convective cell. The measurements used throughout this paper, were obtained near the cloud-top, at temperatures of about $-58\,°$C. During the CIRCLE-2 campaign, the PN instrument was available (Gayet et al., 1998). As the ice crystals enter the sampling volume of the PN, they are intersected by a collimated laser beam, operating at $0.80\,\mu$m, near the focal point of a paraboloidal mirror. A circular array of 54 diodes measures the scattered intensity of laser light scattered at polar angles between $15°$ and $162°$, by each crystal so illuminated. A microphysical probe used during the CIRCLE-2 experiment was the Cloud Particle Imager (CPI) (Lawson et al., 2001). The CPI was used to image the ice crystal habits, and estimate their sizes, example images of the ice crystal habits, imaged near the cloud-top, are shown in Fig. 1a and b.

The figures show that the ice crystal habits appeared to consist of chains of aggregates, with maximum dimensions ranging between about $100\,\mu$m to about $400\,\mu$m. Although, the appearance of chain-like aggregates has been previously reported (Saunders and Wahab, 1975; Connolly et al., 2005; Um and McFarquhar, 2009; Baran, 2009; and Gayet et al., 2012), their corresponding phase functions have not generally been measured, until Gayet et al. (2012). Due to the differing sampling volumes of the PN and CPI instruments,
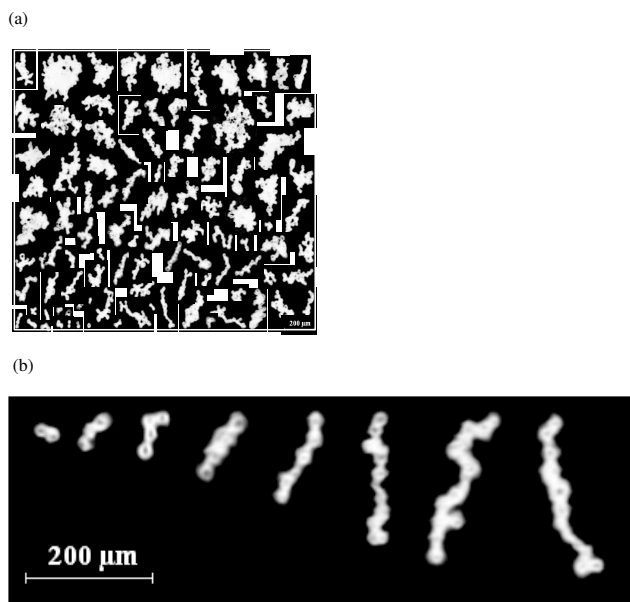
(a)

(b)

200 µm

Fig. 1. (a) CPI example images of ice crystal chain-aggregates that occurred near the cloud-top of an overshooting mid-latitude anvil, obtained during the CIRCLE-2 experiment. The ice crystal size is shown by the scale located at the bottom-right-hand-side of the figure. From Gayet et al. (2012), see their Fig. 8. **(b)** A higher resolution image of **(a)** showing typical examples of the chain-like aggregates that occurred in the anvil. The ice crystal size is shown by the scale located at the bottom-left-hand-side of the figure. From Gayet et al. (2012), see their Fig. 10.

these instruments do not measure the same ice crystals. They do however, measure ice crystals, which occurred in the same cloud. It is therefore, possible, to make statistical comparisons between the CPI and PN measurements, over the same population of ice crystals. The PN measured-averaged phase function, near the cloud-top, shown in Fig. 7c of Gayet et al. (2012), is a statistical representation of the phase functions, produced by a similar population of ice crystals as shown in Fig. 1a and Fig. 1b. The PN estimated-averaged asymmetry parameter was estimated by Gayet et al. (2012) to be 0.78 ± 0.04.

In the paper by Gayet et al. (2012), it is shown that the measured-averaged phase function, at scattering angles less than about $100°$, is featureless. Which corresponds to previous literature that the measured scattered intensity of more complex aged ice crystals do not exhibit halo features, around the scattering angles of $22°$ and $46°$ (Field et al., 2003; Ulanowski et al., 2011; Gayet et al., 2011, 2012). However, at scattering angles between about $120°$ and $160°$, there appears a bow-like feature. As previously mentioned, the appearance of bow-like features on the phase function, at backscattering angles, is contrary to the general radiometric measurements discussed in Sect. 1. Moreover, Gayet et al. (2012) also noted the presence of quasi-spherical ice particles with diameters between about $15 \, \mu m$ and $20 \, \mu m$ that

made up some of the aggregate-chains. The possibility of the bow-like feature being due to the quasi-spherical ice particles rather than the non-spherical ice crystal aggregate is discussed in Sect. 4.

3 Theoretical methodology

To interpret the phase function reported by Gayet et al. (2012), a number of light scattering methods are used. Firstly, in the rest of this paper, the ice crystals are assumed to be randomly oriented, and monodispersive. The incident wavelength is $0.80 \, \mu m$. The refractive index of ice at this wavelength is $1.3049 + i 1.34 \times 10^{-7}$ (Warren and Brandt, 2008), where i is the imaginary part.

To compute the scattering phase function (first element in the first column of the scattering matrix [1,1], see van de Hulst, 1957), $P_{11} (\theta)$, for each ice crystal, the methods of Monte-Carlo ray tracing (Macke et al., 1996a) and T-matrix (Mishchenko and Travis, 1998) are applied. The method of ray-tracing is applied to a model chain of aggregates, and the T-matrix method is applied to rotationally symmetric particles, which represent the quasi-spherical ice particles. Since no halo features are noted on the averaged phase function reported by Gayet et al. (2012), the method of distortion is applied to the ray tracing (Macke et al., 1996a; Yang and Liou, 1998). In this method, at each refraction and reflection event, the ray-paths are randomly tilted, with respect to their original direction. This randomization process removes energy from the halo and ice bow regions and re-distributes it to side-scattering and backscattering angles. Therefore, for high distortion parameters, the halo and ice bow features are removed, creating featureless phase functions. The distortion parameter can have values ranging from 0 (i.e., no distortion) to 1.0 (i.e., maximum distortion).

This geometric method of distortion is commonly referred to, in the literature, as surface roughness, as it is supposed to mimic scattering from the smaller-scale structure that might occur on the surfaces of ice crystals. Since, neither Geometric nor Physical Optics can be applied to such small-scale structures, due to diffractive effects that would originate from the smaller-scale structures; a large-scale geometric method of distortion is used to approximate the small-scale structure. How well such geometric methods represent scattering, due to actual surface roughness, has yet to be evaluated, since to date, there have been no comparisons between the distortion approximation and electromagnetic theory. Due to this lack of evidence, in this paper, the term distortion is used rather than surface roughness. Another method that can be applied to remove halos and ice bows is including ice crystals with aerosols or air bubble inclusions (Macke et al., 1996b and Labonnote et al., 2001) or a combination of distortion and spherical air bubble inclusions (Baran and Labonnote, 2007). These methods of randomization decrease the asymmetry parameter of the model ice crystal, with respect to their

pristine counterparts (Macke et al., 1996a; Yang and Liou, 1998; Ulanowski et al., 2006).

In this paper, the chains of non-spherical ice aggregates shown in Fig. 1a are represented by a ten-element hexagonal ice aggregate, previously described by Baran and Labonnote (2007), see Fig. 1f of that paper. The ten-element aggregate chain is chosen, as this chain is spatial rather than compact, in Fig. 1b; the aggregate chain also appears spatial rather than compact, and in that figure the chain appears to be composed of quasi-spherical ice particles. Moreover, the lack of halos being present on the measured phase function reported by Gayet et al. (2012) implies that the aggregate-chain has been randomized to such an extent that the initial shapes that compose the aggregates of non-spherical ice crystals are not important. The scattering phase functions of such highly randomized structures are featureless and relatively flat at backscattering angles (Macke et al., 1996a; Yang and Liou, 1998; Baran et al., 2001; Ulanowski et al., 2006), and so the shape information is lost (Baran et al., 2001). Moreover, the phase function of individual ice crystals that make up spatial ice aggregates is very similar to the phase function of the aggregate ice crystal, due to multiple reflections between the individual monomers that make up the spatial aggregate being unimportant (Um and McFarquhar, 2009; Baran, 2009).

The appearance of ice bow-like features on the scattering phase function at backscattering angles is usually indicative of regular ice crystals (Takano and Liou, 1989) or ice spheres or quasi-spherical ice particles (Mugnai and Wiscombe, 1986; Mishchenko and Travis, 1998). It has been previously argued that the underlying ice crystal shape is unimportant due to the processes of randomization leading to featureless phase functions. Therefore, the ice bow-like feature reported by Gayet et al. (2012) is due to either ice spheres or quasi-spherical ice particles. In this paper, the quasi-spherical ice particles are represented by rotationally symmetric ice spheroids and Chebyshev ice particles. The geometries of these particles have previously been described by (Mugnai and Wiscombe, 1986; Mishchenko and Travis, 1998). In those papers, it is shown that high-order Chebyshev particles with high deformation parameters and spheroids of large aspect ratio do not support ice-bow like features on their scattering phase functions. Therefore, to retain the ice bow-like feature, the Chebyshev ice particles and ice spheroids are assumed to be of low order and low aspect ratio, respectively. However, in this paper, the choice of geometry chosen to represent the quasi-spherical particles is not claimed to be unique, rather, that the ice bow-like feature reported by Gayet et al. (2012), can be explained by either the ice sphere or some quasi-spherical ice particle. With this in mind, the following geometrical parameters are assumed to represent the quasi-spherical ice particles.

The aspect ratios (i.e., the ratio of horizontal semi-axis to the rotational semi-axis), R, of the prolate and oblate spheroids are assumed to be 0.8333 and 1.2 (R as defined by
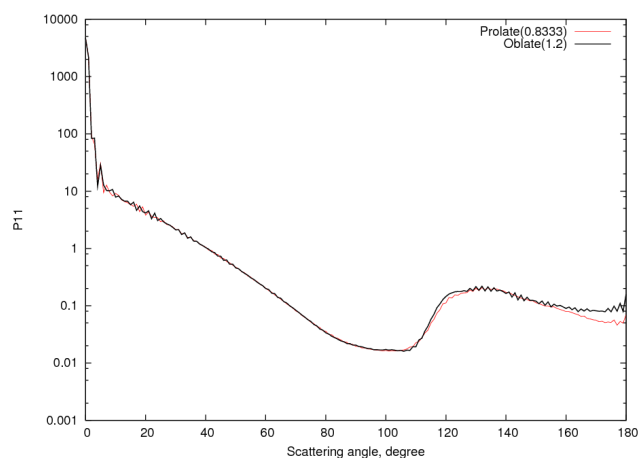

Fig. 2. The normalised scattering phase function plotted against scattering angle, calculated for the prolate spheroid of aspect ratio 0.8333 (red line) and oblate spheroid of aspect ratio 1.2 (black line).

Mishchenko and Travis, 1998), respectively, and the equal-area spherical radius is assumed to be 12 μm, which is close to the upper end of the in-situ estimate of the quasi-spherical ice particle radius (Gayet et al., 2012). An equal area spherical radius of 7.5 μm was also assumed, but the phase functions for particles of this size, were not significantly different from those assuming a radius of 12 μm (not shown for reasons of brevity). The normalized scattering phase functions of the prolate and oblate spheroids are shown in Fig. 2. The figure shows, that these assumed aspect ratios for the spheroids, exhibit ice bow-like features at scattering angles between about 110° and 150°, peaking at scattering angles between about 125° and 135°. The peak of the ice bow-like feature reported by Gayet et al. (2012) occurs at a scattering angle of about 140°. The prolate spheroid scattering phase function slightly shifts the peak of the ice bow towards the peak of the measured in-situ ice bow-like feature, and has lower backscattering than the oblate spheroid, at scattering angles between about 150° and 180°. However, both the prolate and oblate scattering phase functions exhibit low side-scattering, which is typical of quasi-spherical particles (Mishchenko and Travis, 1998). Other higher and lower aspect ratios were investigated, but these tended to either smooth the ice-bow feature or move it to lower scattering angles, towards the sphere bow, at the rainbow angle of 138°, respectively (not shown here for reasons of brevity).

High order Chebyshev ice particles have been previously assumed by McFarquhar et al. (2002) to represent the scattering properties of small individual ice crystals of dimensions less than 100 μm. For dimensions greater than this, other idealized geometrical shapes were assumed, such as rough and smooth hexagonal ice aggregates (Yang and Liou, 1998), pristine hexagonal ice columns and plates, bullet rosettes and dendrites. The scattering phase function of the smaller
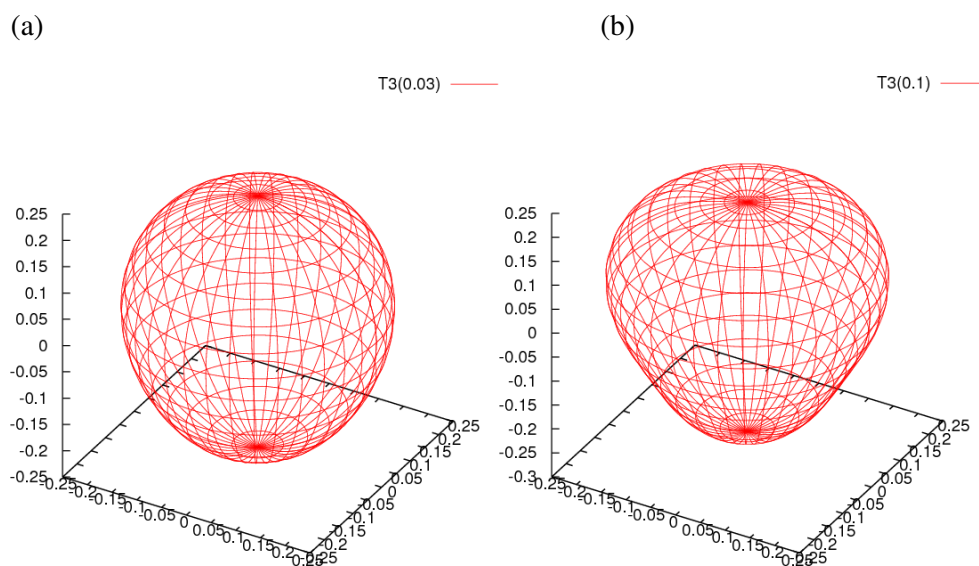
(a)　　　　　　　　　　　　　　　　　　　　(b)

Fig. 3. The shapes of the two Chebyshev particles assumed for the light scattering calculations. **(a)** The Chebyshev particle of order 3 and deformation parameter 0.03 **(b)** The Chebyshev particle of order 3 and deformation parameter of 0.1.
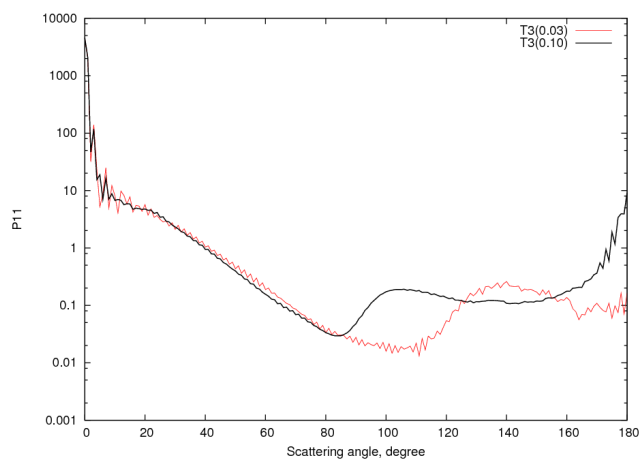

Fig. 4. The normalised scattering phase function plotted against scattering angle, calculated for the Chebyshev particle of order 3 and deformation parameter 0.03, T3(0.03), shown as the red line, and the Chebyshev particle of order 3 and deformation parameter 0.1, T3(0.10), shown as the black line.

Chebyshev ice crystals were merged with the larger ice crystals, using in-situ derived particle size distributions, to predict the averaged single-scattering properties of cirrus at various wavelengths in the solar region. The merged averaged non-absorbing scattering phase function (see Fig. 4a and b of Mc-Farquhar et al. 2002) was essentially featureless around the ice-bow region. As previously indicated, higher aspect ratio spheroids or high-order Chebyshev particles tend to smooth the scattering phase function (Mishchenko and Travis, 1998). In order to retain the ice-bow feature, in this paper, the Chebyshev particles are assumed to be of order 3, have an

unperturbed spherical radius of 12 µm, and deformation parameters of 0.03, and 0.1. Hereinafter, the two Chebyshev particles are described by the term T$n(\varepsilon)$, where n is the Chebyshev order, and ε is the deformation parameter, as defined by Mishchenko and Travis (1998). The shapes of the Chebyshev particles are shown in Fig. 3a and b, and their scattering phase functions are shown in Fig. 4. The scattering phase function of the Chebyshev particle T3(0.03) exhibits an ice bow-like feature, and it peaks at the scattering angle of about 140°, which is very similar to the peak of the in-situ measured ice bow-like feature. The Chebyshev ice particle with a higher deformation parameter smoothes the phase function around the ice bow region but moves the feature to side-scattering angles, between the scattering angles of about 80° and 100°. Lower order Chebyshev ice particles were also investigated but these, moved the ice bow region to the sphere rainbow angle (not shown here for reasons of brevity). Clearly, as shown by Figs. 3 and 4, the quasi-spherical ice particles cannot, by themselves, re-produce the side scattering reported by Gayet et al. (2012). As a consequence, these particles must be merged with highly randomized ice crystals to satisfactorily account for the side-scattering reported by Gayet et al. (2012).

Therefore, to simulate the measured averaged phase functions, four weighted habit mixture models are investigated. Moreover, a weighted habit mixture model is assumed because, currently, there is no one single electromagnetic method that can solve the scattering properties of chain aggregates for the dimensions shown in Fig. 1a and b.

The first weighted habit mixture model is comprised of the two previously described Chebyshev ice particles, called model 1. The second model consists of the highly

randomized ten-element hexagonal ice aggregate and ice spheres, called model 2. The effective radius of the ice sphere was assumed to be 12 μm. Due to significant interference on the scattering phase function of the sphere (Mishchenko and Travis, 1998), the predicted phase function is integrated over a very narrow particle size distribution, in order to smooth its scattering phase function, so that a clear comparison can be made between the model and the in-situ measurements. The particle size distribution assumed was the log-normal (see Mishchenko and Travis, 1998) and the sphere scattering phase functions were integrated between the radii of 11.88 and 12.12 μm. The third model consists of the highly randomized ten-element hexagonal ice aggregate and the two previously described spheroids, called model 3. The fourth model consists of the highly randomized ten-element hexagonal ice aggregate and the two previously described Chebyshev ice particles, called model 4.

The normalised scattering phase function is given by the following relation (Bohren and Huffman, 1983)

$$\frac{1}{4\pi} \int_{4\pi} P_{11} d\Omega = 1 \qquad (1)$$

where in Eq. (1) P_{11} is the previously defined single-scattering phase function. The asymmetry parameter was defined as the average cosine of the scattering angle, and is given by the following relation (Bohren and Huffman, 1983)

$$g = \langle \cos\theta \rangle = \frac{1}{2} \int_0^\pi P_{11}(\theta) \cos\theta \sin\theta d\theta. \qquad (2)$$

To compare P_{11} directly to the in-situ measurements, i.e., the differential scattering cross section, would require knowledge of the total scattering cross section and total number density of ice particles. However, due to the problem of ice crystal shattering on the inlets of closed-path microphysical instruments (Korolev et al. 2011), there is considerable uncertainty with regard to the actual values of the total number concentration and volume extinction coefficient. To achieve direct comparisons between theory and measurements would also require better in-situ microphysics with shattering effects removed. Also, more detailed information is also required on the distribution and shapes (i.e., aspect ratios) of the individual structures that compose the ice aggregates. Therefore, in this paper, true closure is not claimed, since in-situ measurements are not currently available that meet the above-mentioned closure requirements.

In this paper, the overall shape of the scattering phase function and its associated asymmetry parameter are the quantities of interest, and Fig. 1a or b, does not show any evidence of shattering. It is assumed that the measured phase functions are unaffected by shattering. Therefore, the model phase functions are scaled, until the best overall fit to the in-situ measurements is obtained. The best-fit model phase

function (normalized to 4π) is then applied to Eq. (2) to estimate the asymmetry parameter.

The weighted mean phase function, $\overline{P_{11}(\theta)}$, is given by:

$$\overline{P_{11}(\theta)} = \sum_{j=1}^{J=N} w_j P_j \qquad (3)$$

where in Eq. (3) w_j is the weighting applied to each phase function, and by definition $\Sigma w_j = 1$. In Eq. (3), the weights are found by minimizing the root mean square error (rmse), X_{rmse}, which is defined by

$$X_{\text{rmse}} = \sqrt{(1/N) \left\{ \sum_{i=1}^{i=32} X_i^2 \right\}} \qquad (4)$$

where in Eq. (5), X_i is the difference between the in-situ measured average phase function and $\overline{P_{11}(\theta)}$, where $i = 1 \ldots N$, and $N = 32$ (i.e., the number of scattering angles measured by the PN). The results of comparing the four models with the in-situ measurements of the phase functions are described in the next section.

4 Results

Considering model 1, and using Eqs. (3) and (4), to obtain the weights that best minimise differences between theory and measurement, the best weighted mean habit mixture model was found to be

$$\overline{P_{11}} = 0.4 P_{11}^{T3(0.03)} + 0.6 P_{11}^{T3(0.1)} \qquad (5)$$

where i has been dropped for reasons of clarity. The rmse, with the above weights, was found to minimize to a value of 1.1×10^{-7}. Comparisons between $\overline{P_{11}}$ and the in-situ measured phase function are shown in Fig. 5. In all figures, the model predicted phase function is shown over all scattering angles. The full model scattering phase function is plotted, to demonstrate that in order to discriminate between models, PN instruments that measure the scattered intensity over a more complete range of scattering angle are required.

Figure 5 shows that for scattering angles between about 15° and less than 60°, model 1 overpredicts the forward scattering part of the measured phase function. However, at side-scattering angles between about 60° and less than 100°, the model severely underpredicts the measurements. However, the ice bow feature, between the scattering angles of 120° and 160°, is predicted by the Chebyshev particle model. On inspection, the overall fit to the in-situ measurements is poor. Therefore, Fig. 5 demonstrates that quasi-spherical particles alone cannot explain the measured phase function. Moreover, g predicted by model 1 is 0.84, which is outside the upper range of uncertainty estimated by the PN. A phase function with higher side scattering is required, without halo features, which can only be predicted by an irregular ice crystal model.
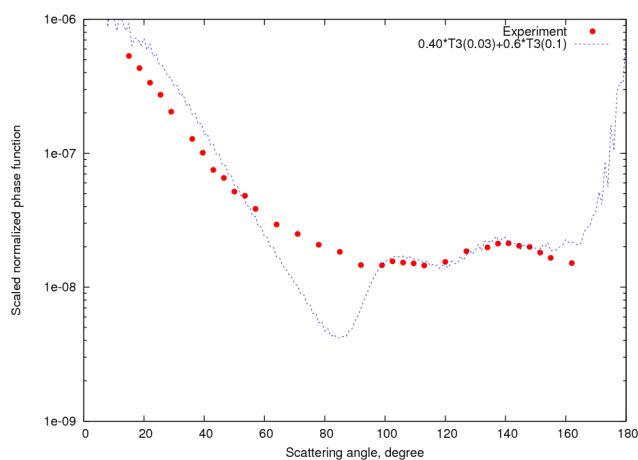
Fig. 5. The scaled normalized scattering phase function plotted against the scattering angle. Showing, the PN measured average phase function (filled red circles) and weighted habit mixture model 1 (0.4·T3 (0.03)+0.6·T3 (0.1)), which is represented by the blue dashed line.

Fig. 6. Same as Fig. 5 but for the weighted habit mixture model 2 (0.3·C+0.7·Sphere).

To obtain a phase function with higher side scattering, without halo features, the highly distorted ten element hexagonal ice aggregate is now considered. To reduce the noise in the Monte-Carlo ray tracing calculations for each phase function, the phase functions were averaged over four maximum dimensions, which were 100 μm, 200 μm, 400 μm and 600 μm. For each maximum dimension, the overall aspect ratio of the ten element hexagonal ice aggregate remained invariant with respect to size. A distortion parameter of 0.8 was assumed for all four Monte-Carlo ray tracing calculations. Although lower distortion parameters were tried these did not minimize the rmse as well as the distortion parameter of 0.8 (these results are not shown here for reasons of brevity). It should be noted here, that the averaged g value found for the highly distorted ten element hexagonal ice aggregate was 0.68.

Considering model 2, the best weighted mean habit mixture model was found to be

$$\overline{P_{11}} = 0.3P_{11}^{\text{ice aggregate}} + 0.7P_{11}^{\text{sphere}}. \tag{6}$$

The rmse, with the above weights, was found to minimize to a value of 1.6×10^{-8}.

The results of comparing the phase function with the measured phase function are shown in Fig. 6. Clearly, the figure shows that the addition of the highly distorted ten element hexagonal ice aggregate has improved the fit between model 2 and the measured phase function, relative to model 1, especially between the scattering angles of about 40° and 100°. However, beyond the scattering angle of 100°, not surprisingly, the peak in the phase function occurs at the rainbow angle of 138°, and the width of the peak is narrower than the ice bow-like feature that is apparent on the in-situ measured phase function. Therefore, assuming spheres, cannot
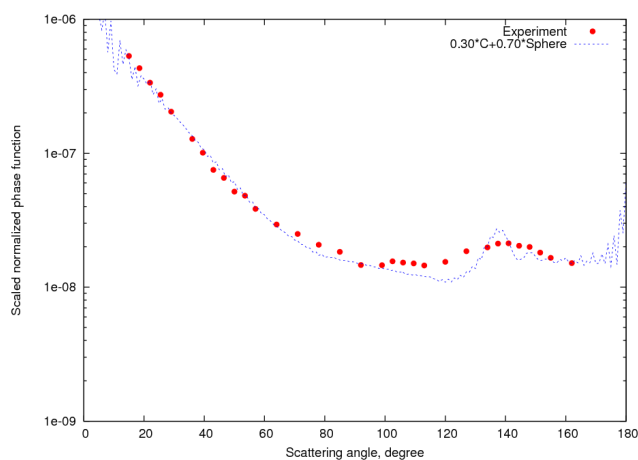
account for the in-situ measurements of the ice bow-like feature. However, the model predicted value of the asymmetry parameter is 0.77, which is within the uncertainty of the in-situ estimate. The lower asymmetry parameter predicted by model 2, is due to a reasonable fit to the measurements at forward and side-scattering angles, even though the backscattering angles, beyond about 100°, are not as generally well fitted.

For model 3, the best model fit to the measured phase function was found to be,

$$\overline{P_{11}} = 0.2P_{11}^{\text{ice aggregate}} + 0.3P_{11}^{\text{prolate}(R=0.83333)} + 0.5P_{11}^{\text{oblate}(R=1.2)} \tag{7}$$

and the rmse was found to minimize to a value of 1.4×10^{-8}. Figure 7, shows the model estimated phase function compared against the in-situ measurements. The figure shows an improved fit to the in-situ measurements relative to the assumption of spheres, between the scattering angles of about 90° and 160°, and the rmse for model 3 is lower than model 2. However, the peak in the ice bow assuming spheroids occurs at a scattering angle of about 130°, compared to the measured in-situ peak, which is at about 140°. Between the scattering angles of 160° and less than 180°, the model is relatively flat, but peaks at the exact backscattering angle of 180°, due to the glory feature. The predicted g value for model 3 was found to be 0.80, which is within the upper range of uncertainty estimated by the PN.

For model 4, the best-fit model phase function to the measured phase function was found to be

$$\overline{P_{11}} = 0.2P_{11}^{\text{ice aggregate}+} 0.5P_{11}^{T3(0.03)} + 0.3P_{11}^{T3(0.1)} \tag{8}$$

and the rmse was found to minimize to a value of 1.5×10^{-8}. The comparison between $\overline{P_{11}}$ and the in-situ measurements is shown in Fig. 8. The figure shows that this model better captures, relative to the other models, the shape of the measured phase function between the scattering angles of about 100°
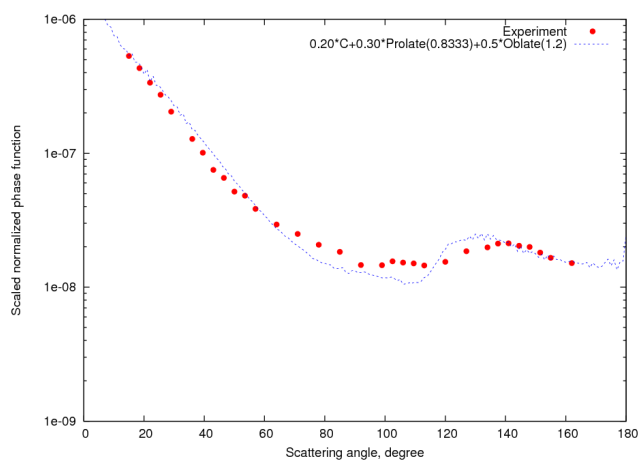
Fig. 7. Same as Fig. 6, but for the weighted habit mixture model 3, $0.2 \cdot C + 0.3 \cdot Prolate(0.8333) + 0.5 \cdot Oblate(1.2)$.
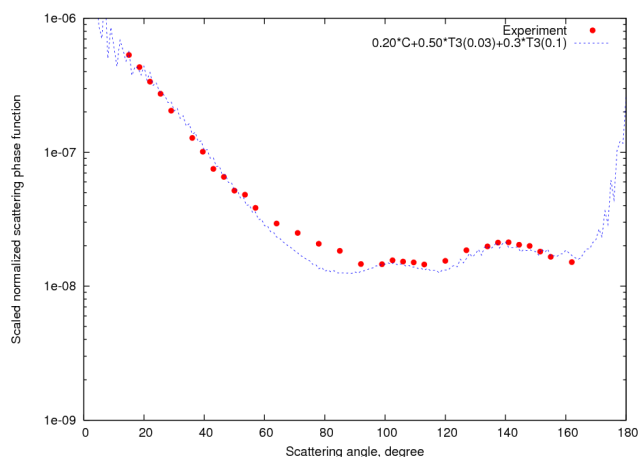

Fig. 8. Same as Fig. 7, but for weighted habit mixture model 4, $0.2 \cdot C + 0.5 \cdot T3 (0.03) + 0.3 \cdot T3 (0.1)$.

and 160°, even predicting the peak of the measured ice bow feature at the correct scattering angle. However, the model slightly underpredicts the measured phase function at scattering angles between about 60° and 95°, and this results in the rmse being slightly higher than model 3. However, overall model 4, better fits the in-situ measurements, considering all scattering angles. However, at scattering angles between 160° and 180° the model retains the strong backscattering feature exhibited by Chebyshev particles. This is in contrast with model 3. This is why it is important to develop future PN instruments that are able to measure the scattered intensity over a more complete range of scattering angle. The predicted g value for model 4 was found to be 0.79, which is within the range of uncertainty estimated by the PN, and slightly higher than model 2, due to its underprediction of the measurements between the scattering angles of about 60° and 95°.

5 Conclusions

In this paper, an unusual in-situ measured scattering phase function has been interpreted in terms of a weighted habit mixture model. The best habit mixture model found to account, overall, for the in-situ measurements, comprised of a highly distorted ten element hexagonal ice aggregate, and two Chebyshev particles of order 3. A distortion parameter of 0.8 was applied to the ten element hexagonal ice aggregate, and the Chebyshev ice particles were each assumed to have an unperturbed spherical radius of 12 µm, and deformation parameters of 0.03 and 0.1, and the best-fit weightings were estimated to be 0.2, 0.5, and 0.3, respectively. The best overall model, has a g value of 0.79, which compares to the estimated PN g-value of 0.78 ± 0.04.

The best overall model demonstrates that the measured ice bow, assuming a highly distorted ice crystal, can be predicted assuming independent quasi-spherical ice particles. Therefore, it is the quasi-spherical ice particles that dominate the backscattering measured by the PN, rather than the non-spherical ice aggregate, although these must be randomized to produce sufficient side-scattering and remove halo features.

Figures 7 and 8 demonstrate that PN instruments are required that measure the scattered intensity over a more complete range of scattering angle, at least as full a scattering angle range that is technically possible. This is required so that discrimination between models and reliable estimates of g can be achieved. Also, further in-situ instrumentation needs to be developed that can image the shapes and aspect ratios of the monomer ice crystals that make up the aggregate ice crystals.

It has been argued in this paper that it is the quasi-spherical ice particles that are responsible for the appearance of the ice bow-like feature on the averaged in-situ measured scattering phase function. In this case, the method of distortion (sometimes referred to as surface roughness) applied to the non-spherical ice aggregate would predict higher side-scattering, relative to the measurements, and no ice bow feature. Consequently, the full scattering phase function of the highly randomized non-spherical ice aggregate, at side-scattering and backscattering angles, is not representative by itself of the measured phase function. In this respect, cloud chamber experiments should be considered, to see, if it is possible, to replicate the conditions necessary to produce similar scattering phase functions reported by Gayet et al. (2012). Moreover, the asymmetry parameter of the best model fit is 16 % higher than the asymmetry parameter predicted by the highly randomised ice aggregate model. Therefore, the asymmetry parameter, in such situations as reported by Gayet et al. (2012), may not necessarily be small.

It can no longer be generally assumed that phase functions with no halos are also featureless and relatively flat at backscattering angles. This may be particularly true for the tops of anvil cloud, and for this type of cloud, g is particularly

important, with regard to climate modelling. To this end, space-based instruments should be developed that can resolve sufficiently, the backscattering properties of cirrus.

The findings of this paper have important implications for cloud physics, climate modelling and for the remote sensing of cirrus. It is therefore, of necessity to understand whether the quasi-spherical ice aggregates, the phase functions, and consequently, their g-values, shown throughout this paper, are a common occurrence.

Edited by: T. Garrett

References

Baran, A. J., Watts, P. D., and Francis, P. N.: Testing the coherence of cirrus microphysical and bulk properties retrieved from dual-viewing multispectral satellite radiance measurements, J. Geophys. Res., 104, 31673–31683, 1999.

Baran, A. J., Francis, P. N., Labonnote, L.-C, Doutriaux-Boucher, M.: A scattering phase function for ice cloud: Tests of applicability using aircraft and satellite multi-angle multi-wavelength radiance measurements of cirrus, Q. J. Roy. Meteor. Soc., 127, 2395–2416, 2001.

Baran, A. J.: On the scattering and absorption properties of cirrus cloud, J. Quant. Spectrosc. Radiat. Transfer, 89, 17–36, 2004.

Baran, A. J.: A review of the light scattering properties of cirrus, J. Quant. Spectrosc. Radiat. Transfer, 110, 1239–1260, 2009.

Baran, A. J.: From the single-scattering properties of ice crystals to climate prediction: A way forward, J. Atmos. Res., 112, 45–69, 2012.

Baran, A. J. and Labonnote, L.-C.: On the reflection and polarization properties of ice cloud, J. Quant. Spectrosc. Radiat. Transfer, 100, 41–54, 2006.

Baran, A. J. and Labonnote, L.-C.: A self-consistent scattering model for cirrus. 1: The solar region, Q. J. Roy. Meteor. Soc., 133, 1899–18912, 2007.

Baum, B. A., Heymsfield, A. J., Yang, P., and Bedka, S. T: Bulk scattering properties for the remote sensing of ice clouds – Part I: Microphysical data and models, J. App. Meteorol., 44, 1885–1895, 2005.

Baum, B. A., Yang, P., Heymsfield, A. J., Schmitt, C. G., Xie, Y., Bansemer, A., Hu, Y.-X., Zhang, Z.: Improvements in Shortwave Bulk Scattering and Absorption Models for the Remote Sensing of Ice Clouds, J. Appl. Meteor. Climatol., 50, 1037–1056, 2011.

Bohren, C. F. and Huffman, D. R.: Absorption and scattering of light by small particles, Wiley, 530 pp., 1983.

Connolly, P. J., Saunders, C. P. R., Gallagher, M. W., Bower, K. N., Flynn, M. J., Choularton, T. W., Whiteway, J., and Lawson, R. P.: Aircraft observations of the influence of electric fields on the aggregation of ice crystals, Q. J. Roy. Meteorol. Soc., 128, 1–19, 2005.

Edwards, J. M., Havemann, S., Thelen J.-C., and Baran, A. J.: A new parametrization for the radiative properties of ice crystals: Comparison with existing schemes and impact in a GCM, Atmos. Res., 83, 19–35, 2007.

Foot, J. S.: Some observations of the optical properties of clouds. II: Cirrus, Q. J. R. Meteor. Soc., 114, 141–164, 1988.

Field, P. R., Baran, A. J., Kaye, P. H., Hirst, E., and R. Greenaway: A test of cirrus ice crystal scattering phase functions, Geophys. Res. Lett., 30, 1752, doi:10.1029/2003GL017482, 2003.

Francis, P. N., Foot, J. S., and Baran, A. J.: Aircraft measurements of the solar and infrared radiative properties of cirrus and their dependence on ice crystal shape, J. Geophys. Res., 104, 31685–31695, 1999.

Fu, Q.: A new parameterization of an asymmetry factor of cirrus clouds for climate models, J. Atmos. Sci., 64, 4140–4150, 2007.

Gayet, J.-F., Auriol, F., Oshchepkov, S., Schröder, F., Duroure, C., Febvre, G., Fournol, J.-F., Crépel, O., Personne, P., and Daugeron, D.: In-situ measurements of the scattering phase function of stratocumulus, contrails and cirrus, Geophys. Res. Lett., 25, 971–974, 1998.

Gayet, J.-F., Mioche, G., Shcherbakov, V., Gourbeyre, C., Busen, R., and Minikin, A.: Optical properties of pristine ice crystals in mid-latitude cirrus clouds: a case study during CIRCLE-2 experiment, Atmos. Chem. Phys., 11, 2537–2544, doi:10.5194/acp-11-2537-2011, 2011.

Gayet, J.-F., Mioche, G., Bugliaro, L., Protat, A., Minikin, A., Wirth, M., Dörnbrack, A., Shcherbakov, V., Mayer, B., Garnier, A., and Gourbeyre, C.: On the observation of unusual high concentration of small chain-like aggregate ice crystals and large ice water contents near the top of a deep convective cloud during the CIRCLE-2 experiment, Atmos. Chem. Phys., 12, 727–744, doi:10.5194/acp-12-727-2012, 2012.

Gu, Y., Liou, K. N., Ou, S. C., and Fovell, R.: Cirrus cloud simulations using WRF with improved radiation parameterization and increased vertical resolution, J. Geophys. Res., 116, D06119, doi:10.1029/2010JD014574, 2011.

I Intergovernmental Panel on Climate Change: Climate Change 2007 – The Physical Science Basis: Contribution of Working Group I to the Fourth Assessment Report of the IPCC, Cambridge University Press, Cambridge, 2007.

Jourdan, O., Oshchepkov, S., Shcherbakov, V., Gayet, J.-F., and Isaka, H.: Assessment of cloud optical parameters in the solar region: Retrievals from airborne measurements of scattering phase functions, J. Geophys. Res., 108, 4572, doi:10.1029/2003JD003493, 2003.

Kristjánsson, J. E., Edwards, J. M., and Mitchell, D. L.: The impact of a new scheme for the optical properties of ice crystals on the climate of two GCMs, J. Geophys. Res., 105, 10063–10079, 2000.

Korolev, A. Emery, V., E. F., Strapp, J. W., Cober, S. G., Isaac, G. A., Wasey, M., and Marcotte, D.: Small ice particles in tropospheric clouds: fact or artifact? Airborne icing instrumentation evaluation experiment, B. Am. Meteorol. Soc., 92, 967–973, doi:10.1175/2010BAMS3141.1, 2011.

Korolev, A., Isaac, G. A., and Hallet, J: Ice particle habits in stratiform cloud, Q. J. Roy. Meteor. Soc., 126, 2873–2902, 2006.

Labonnote, L. C., Brogniez, G., Buriez, J.-C., Doutriaux-Boucher, M., Gayet, J.-F., and Macke, A.: Polarized light scattering by inhomogeneous hexagonal monocrystals. Validation with ADEOS-POLDER measurements, J. Geophys. Res.. 106, 12139–12153, 2001.

Lawson, R. P., Baker, B. A., Schmitt, C. G., and Jensen, T. L.: An overview of microphysical properties of Arctic clouds observed in May and July 1998 during FIRE.ACE, J. Geophys. Res., 106, 14989–15014, 2001.

Liou, K.-N. and Takano, Y.: Light scattering by nonspherical particles: Remote sensing and climatic implications, Atmos. Res., 31, 271–298, 1994.

McFarlane, S. A., Marchand, R. T., and Ackerman, T. P.: Retrieval of cloud phase and crystal habit from Multiangle Imaging Spectroradiometer (MISR) and Moderate Resolution Imaging Spectroradiometer (MODIS) data, J. Geophys. Res., 110, D14201, doi:10.1029/2004JD004831, 2005.

McFarquhar, G. M., Yang, P., Macke, A., and Baran, A. J.: A new parameterization of single scattering solar radiative properties for tropical anvils using observed ice crystal size and shape distributions, J. Atmos. Sci., 59, 2458–2478, 2002.

Macke, A., Mueller, J., and Raschke, E.: Single scattering properties of atmospheric ice crystal, J. Atmos. Sci., 53, 2813–2825, 1996a.

Macke A., Mishchenko, M. I., and Cairns, B.: The influence of inclusions on light scattering by large particles, J. Geophys. Res., 101, 23311–23316, 1996b.

Mishchenko, M. I., Travis, L. D., and Lacis, A. A.: Scattering, Absorption, and Emission of Light by Small particles, Cambridge University Press, Cambridge, 2002.

Mishchenko, M. I. and Travis, L. D.: Capabilities and limitations of a current FORTRAN implementation of the T-matrix method for randomly oriented rotationally symmetric scatterers, J. Quant. Spectrosc. Radiat. Transfer, 60, 309–324, 1998.

Mishchenko, M. I. Rossow, W., Macke, A., and Lacis, A. A.: Sensitivity of cirrus cloud albedo, bidirectional reflectance and optical thickness retrieval accuracy to ice particle shape, J. Geophys. Res., 101, 16973–1698, 1996.

Mugnai, A. and Wiscombe, W. J.: Scattering from nonspherical Chebyshev particles – I: Cross sections, single-scattering albedo, asymmetry factor and backscattering fraction, Appl. Opt. 25, 1235–1244, 1986.

Saunders, C. P. R. and Wahab, N. M. A.: The influence of electric fields on the aggregation of ice crystals, J. Meteorol. Soc. Jpn., 53, 121–126, 1975.

Stephens, G. L. and Webster, P. J.: Clouds and Climate: Sensitivity of Simple Systems. J. Atmos. Sci., 38, 235–245, 1981.

Takano, Y. and Liou, K. N, Solar radiative transfer in cirrus cloud – Part I: single-scattering and optical properties of hexagonal ice crystals, J. Atmos. Sci., 46, 3–19, 1989.

Ulanowski, Z., Kaye, P. H., Hirst, E. and Greenaway, R.: Retrieving the size of particles with rough surfaces from 2D scattering patterns. *13th Int. Conf. Electromagn. Light Scatt., Taormina,* 2011.

Ulanowski, Z., Hesse, E., Kaye, P. H., and Baran, A. J.: Light scattering by complex ice-analogue crystals, J. Quant. Spectrosc. Radiat. Transfer, 100, 382–392, 2006.

Um, J. and McFarquhar, G. M.: Single-scattering properties of aggregates plates, Q. J. Roy. Meteor. Soc., 135, 291–304, 2009.

van de Hulst, H. C.: Light Scattering by Small Particles, Wiley, New York, USA, 470 pp., 1957.

Warren, S. G. and Brandt, R. E.: Optical constants of ice from the ultraviolet to the microwave: A revised compilation, J. Geophys. Res., 113, D14220, doi:10.1029/2007JD009744, 2008.

Yang., P., Zhang, Z. B., Kattawar, G. W.,Warren, S. G., Baum, B. A., Huang, H. J., Hu, Y. X., Winker, D., and Iaquinta, J.: Effect of cavities on the optical properties of bullet rosettes: Implications for active and passive remote sensing of ice cloud properties, J. Appl. Meteor. Climatol., 47, 2311–2330, 2008.

Yang, P. and Liou, K. N.: Single-scattering properties of complex ice crystals in terrestrial atmosphere, Contr. Atmos. Phys., 71, 223–248, 1998.

Zhang, Y., Macke, A., and Albers, F.: Effect of crystal size spectrum and crystal shape on stratiform cirrus radiative forcing, Atmos. Res, 52, 59–75, 1999.